

Resonant manifestations of chiral excitons in Faraday and Kerr effects in a topological insulator filmD. K. Efimkin¹ and Yu. E. Lozovik^{1,2,*}¹*Institute of Spectroscopy RAS, 142190, Troitsk, Moscow Region, Russia*²*Moscow Institute of Physics and Technology, 141700, Moscow, Russia*

(Received 15 August 2012; revised manuscript received 6 April 2013; published 13 June 2013)

Manifestations of chiral excitons on a magnetically gapped surfaces of a topological insulator thin film in Kerr and Faraday effects are analyzed. Excitonic contribution to a surface optical conductivity tensor is calculated. Chiral excitons contrary to conventional ones resonantly contribute to Hall conductivity due to the lack of symmetry between the states with opposite angular momentum. They can lead to the considerable enhancement of Faraday angle and ellipticity of transmitted electromagnetic wave. Chiral excitons cause a decrease of Kerr angle and prominent signatures in ellipticity of reflected electromagnetic wave. Conditions for experimental observation of the described effects are discussed.

DOI: [10.1103/PhysRevB.87.245416](https://doi.org/10.1103/PhysRevB.87.245416)

PACS number(s): 73.21.-b, 78.67.-n, 33.57.+c

I. INTRODUCTION

Theoretical and experimental study of topological insulators (TIs) that have nontrivial topology intrinsic to their band structure grows rapidly (see Refs. 1,2, and references therein). TIs have a forbidden band in a bulk but on their surface (three dimensional) or edge (two dimensional) there are very unusual electronic states. Recently a “new generation” of three-dimensional (3D) topological insulators (the compounds Bi₂Se₃, Bi₂Te₃, and others), retaining topologically protected behavior at room temperature, were investigated experimentally.³⁻⁵ The surface states of these materials are protected from nonmagnetic disorder and obey the Dirac equation for massless two-dimensional (2D) particles that is analogous to one for electrons in graphene, a unique two-dimensional carbon based material with extraordinary electronic and mechanical properties.⁶⁻⁸

Interesting physics arise when time reversal symmetry on the surface of a TI is broken by an external exchange field. An exchange field that can be created by ordered magnetic impurities introduced to a TI bulk^{9,10} acts only on the magnetic moment of the electrons and generates the energetic gap in the surface spectrum. Contrary to the initial gapless state, the set of excitonic states appears in the gap due to Coulomb interaction on the surface. It is interesting that the excitonic state has minimal energy at a finite value of orbital angular momentum quantum number and can be called “chiral.”¹¹

The time reversal symmetry breaking leads to half-integer quantization of the surface Hall conductivity and, as a result, to quantized Faraday and Kerr effects on the surface of a TI.¹²⁻¹⁵ If the time reversal symmetry is broken on the whole surface of a TI, low frequency electromagnetic response of TI bulk can be described by a *macroscopic* approach based on Lagrangian for an electromagnetic field with an additional θ -term that corresponds to a topological magnetoelectric effect.^{16,17} The topological magnetoelectric effect in TI bulk provides a solid state realization of axion electrodynamics.¹⁸ In the thin film of a TI, which width is considerably smaller than the length of the incident electromagnetic wave, Faraday angle θ_F and Kerr angle θ_K are universal: $\tan \theta_F = \alpha$ and $\tan \theta_K = 1/\alpha$, where $\alpha \approx 1/137$ is the fine structure constant. Within the *macroscopic* approach the roles of oblique incidence of electromagnetic wave,¹³ substrate,¹² and interference in

thick TI film¹³ were theoretically investigated. In spite of its mathematical elegance, this approach is well justified only in the low frequency limit and does not allow to take into account the frequency dispersion effects and many-body correlations on the TI surface.

There is another approach for investigation of the effects on a TI surface based on the Maxwell equations. Response of a TI surface in this approach is characterized by the *microscopically* calculated optical conductivity tensor. The role of frequency dispersion of the optical conductivity was investigated for TI films subjected to an external exchange field.¹⁵ Also the inverse Faraday effect that manifests itself as a generation of spin polarization under illumination of circularly polarized electromagnetic wave was considered.¹⁹ But the manifestation of collective excitations—excitons in Faraday and Kerr effects has not been considered before.

Here we theoretically investigate the role of chiral excitons on a TI surface with a magnetically induced gap in Faraday and Kerr effects.

The rest of the paper is organized as follows. In Sec. II we briefly discuss the electronic structure of a TI surface with a magnetically induced gap. Section III is devoted to a descriptions of chiral excitons. In Sec. IV the contribution of chiral excitons to optical conductivity is calculated. Section V is devoted to Faraday and Kerr effects in thin films of TI. Section VI is devoted to conclusions.

II. ELECTRONIC STRUCTURE OF TIs

Electrons populating the surface states of a TI in the presence of the external exchange field can be described by the following single particle Hamiltonian^{1,2}:

$$H_0 = v_F \mathbf{n}[\mathbf{k} \times \boldsymbol{\sigma}] + \Delta \sigma_z, \quad (1)$$

where v_F is the Fermi velocity of the electron; the vector $\boldsymbol{\sigma} = (\sigma_x, \sigma_y)$ consists of Pauli matrices acting in the space of its spin projections; and Δ parametrizes the coupling of the z component of the exchange field to that of the electron spin. Other components of the exchange field can be excluded by gauge transformation that shifts the Dirac point in momentum space. It can be shown that the magnetic field caused by a layer of ordered magnetic impurities is small and its effect on the

Dirac electrons can be neglected. The spectrum $E_{\mathbf{k}\gamma} = \gamma \epsilon_{\mathbf{k}} = \gamma \sqrt{|\Delta|^2 + v_F^2 k^2}$ is formed by conduction ($\gamma = 1$) and valence ($\gamma = -1$) bands separated by the gap $2|\Delta|$. Corresponding eigenfunctions of the Hamiltonian (1) can be written as $e^{i\mathbf{k}\mathbf{r}}|f_{\mathbf{k}\gamma}\rangle$, where $|f_{\mathbf{k}\gamma}\rangle$ is a spinor part of the wave function:

$$|f_{\mathbf{k}\gamma}\rangle = \begin{pmatrix} \cos(\theta_{\mathbf{k}\gamma}/2)e^{-i\varphi_{\mathbf{k}}/2} \\ i \sin(\theta_{\mathbf{k}\gamma}/2)\gamma e^{i\varphi_{\mathbf{k}}/2} \end{pmatrix}, \quad (2)$$

where $\cos(\theta_{\mathbf{k}\gamma}) = \gamma \Delta / \epsilon_{\mathbf{k}}$, and $\varphi_{\mathbf{k}}$ is polar angle for momentum vector \mathbf{k} .

A starting point for the description of the chiral excitons is the many-body Hamiltonian describing interacting electrons on the surface of the TI:

$$H = \sum_{\mathbf{k}\gamma} \epsilon_{\mathbf{k}\gamma} a_{\mathbf{k}\gamma}^+ a_{\mathbf{k}\gamma} + \frac{1}{2} \sum_{\mathbf{q}\mathbf{k}} \sum_{\substack{\gamma_1 \gamma_2 \\ \gamma'_1 \gamma'_2}} V_c(\mathbf{q}) \langle f_{\mathbf{k}+\mathbf{q}, \gamma'_1} | f_{\mathbf{k}\gamma_1} \rangle \times \langle f_{\mathbf{k}'-\mathbf{q}, \gamma'_2} | f_{\mathbf{k}'\gamma_2} \rangle a_{\mathbf{k}+\mathbf{q}, \gamma'_1}^+ a_{\mathbf{k}'-\mathbf{q}, \gamma'_2}^+ a_{\mathbf{k}'\gamma_2} a_{\mathbf{k}\gamma_1}, \quad (3)$$

where $a_{\mathbf{k}\gamma}$ is the destruction operator for an electron with momentum \mathbf{k} from the band γ ; $V_c(\mathbf{q}) = 2\pi e^2 / \epsilon q$ is the two-dimensional Fourier transform of the Coulomb interaction potential; and ϵ is the effective dielectric permittivity of the TI surface.

III. CHIRAL EXCITONS

Coulomb interaction between electrons populating surface states of the TIs can lead to formation of excitons that manifest themselves as coherent superposition of interband single-particle transitions and can be represented as a bound state of an electron from the conduction band and a hole from the valence band. A creation operator of exciton $d_{\mathbf{q}}^+$ with center of mass momentum \mathbf{q} can be written as²⁰

$$d_{\mathbf{q}}^+ = \sum_{\mathbf{k}} C_{\mathbf{k}\mathbf{q}} a_{\mathbf{k}+\mathbf{q}, 1}^+ a_{\mathbf{k}, -1}, \quad (4)$$

where the set of coefficients $C_{\mathbf{k}\mathbf{q}}$ forms the wave function of an electron and hole forming exciton in the momentum representation. We considered excitons with zero center of mass momentum $\mathbf{q} = 0$ because only they are optically active. Hence, momentum index \mathbf{q} will be omitted below.

Within the equation of motion based approach^{11,20} excitons can be represented as composite bosons with corresponding commutation relation $[d, d^+] = 1$ and their creation operator satisfies the equation of motion $[H, d^+] = \Omega d^+$, where Ω is exciton energy and H is the Hamiltonian of interacting electrons (3). If the part of the Coulomb interaction in (3) that corresponds to scattering of electrons within a single band is treated within Hartree-Fock approximation, the equation of motion for the excitonic creation operator leads to

$$(2\epsilon_{\mathbf{k}} + \Sigma_{\mathbf{k}}^{\text{eh}})C_{\mathbf{k}} + \sum_{\mathbf{k}'} V_c(\mathbf{k} - \mathbf{k}') \Lambda_{\mathbf{k}, \mathbf{k}'} C_{\mathbf{k}'} = \Omega C_{\mathbf{k}}, \quad (5)$$

where $\Sigma_{\mathbf{k}}^{\text{eh}}$ is the self-energy of the electron-hole pair and $\Lambda_{\mathbf{k}, \mathbf{k}'}$ is an angular factor that are given by

$$\begin{aligned} \Sigma_{\mathbf{k}}^{\text{eh}} &= \sum_{\mathbf{k}'} V_c(\mathbf{k} - \mathbf{k}') \frac{\Delta^2 + v_F^2(\mathbf{k} \cdot \mathbf{k}')}{\epsilon_{\mathbf{k}} \epsilon_{\mathbf{k}'}} \\ \Lambda_{\mathbf{k}, \mathbf{k}'} &= \frac{1}{2} \frac{v_F^2 k k'}{\epsilon_{\mathbf{k}} \epsilon_{\mathbf{k}'}} + \frac{1}{2} \left(1 + \frac{\Delta^2}{\epsilon_{\mathbf{k}} \epsilon_{\mathbf{k}'}} \right) \cos(\phi_{\mathbf{k}} - \phi_{\mathbf{k}'}) \\ &\quad + \frac{i}{2} \left(\frac{\Delta}{\epsilon_{\mathbf{k}}} + \frac{\Delta}{\epsilon_{\mathbf{k}'}} \right) \sin(\phi_{\mathbf{k}} - \phi_{\mathbf{k}'}). \end{aligned} \quad (6)$$

Equation (5) was derived and solved numerically in Ref. 11. The set of excitonic states in the surface gap has an unusual dependence on the orbital angular momentum m and can be called ‘‘chiral.’’ A chiral exciton has minimal energy at a finite value of the orbital angular momentum $m = 1$ and there is no symmetry between chiral excitonic states with opposite angular momenta. The sign of the orbital angular momentum that corresponds to the lowest-energy state depends on the sign of Δ and hence on direction of the exchange field. Chiral excitons also appear²¹ in bilayer graphene gapped by an external electric field.^{22–24} In bilayer graphene chiral excitons with minimal energy have orbital angular momentum $m = 2$.

Here we develop an analytical approximate solution of (5). Self-energy $\Sigma_{\mathbf{k}}^{\text{eh}}$ only renormalizes parameters of single particle spectrum Δ, v_F . If we denote by Δ, v_F the renormalized parameters of the spectrum, then the self-energy term in (5) can be omitted. Angular factor $\Lambda_{\mathbf{k}, \mathbf{k}'}$ and single particle spectrum $\epsilon_{\mathbf{k}}$ contain the single scale $k_{\Delta} = |\Delta|/v_F$ that corresponds to crossover between linear and parabolic regimes of the massive Dirac spectrum. If localization length k_{exc} of the wave function of the relative motion in momentum space $C_{\mathbf{k}}$ satisfies condition $k_{\text{exc}} \ll k_{\Delta}$, single particle energy and the angular factor can be approximated in the following way: $\epsilon_{\mathbf{k}} \approx |\Delta| + v_F^2 k^2 / 2|\Delta|$ and $\Lambda_{\mathbf{k}, \mathbf{k}'} \approx \cos(\phi_{\mathbf{k}} - \phi_{\mathbf{k}'}) + i \sin(\phi_{\mathbf{k}} - \phi_{\mathbf{k}'})$. In this limit Eq. (5) coincides with Schrödinger equation for a 2D hydrogen atom in which: (1) Multipole momenta of Coulomb potential Fourier transform are *shifted* by $\delta m = 1$ due to the angular factor $\Lambda_{\mathbf{k}, \mathbf{k}'} = e^{i(\phi_{\mathbf{k}} - \phi_{\mathbf{k}'})}$; and (2) an effective reduced mass of electron in a 2D hydrogen atom problem is $\mu^* = |\Delta|/2v_F^2$. The chiral excitons can be characterized by radial $n = 0, 1, \dots$ and orbital angular $m = 0, \pm 1, \dots$ quantum numbers with $|m - 1| \leq n$. Their energy spectrum Ω_{nm} and wave functions in momentum space $C_{\mathbf{k}}^{nm}$ can be obtained by a *shift* of well-known ones for a 2D hydrogen atom. Energy of the excitonic level $|n, m\rangle$ is given by

$$\Omega_{nm} = 2|\Delta| - \frac{\alpha_c^2 |\Delta|}{(2n + 1)^2}, \quad (7)$$

where $\alpha_c = e^2 / \epsilon \hbar v_F$ is the dimensionless coupling strength. State $|0, 1\rangle$ with minimal energy has orbital angular momentum $m = 1$. Bohr radius of the chiral exciton and corresponding Rydberg energy are $(\alpha_c k_{\Delta})^{-1}$ and $\alpha_c^2 |\Delta|$. Characteristic momentum k_{exc} of excitonic wave function $C_{\mathbf{k}}$ localization in momentum space can be estimated as an inverse Bohr radius and is equal to $k_{\text{exc}} = \alpha_c k_{\Delta}$. Therefore the shifted eigenstates of the Schrödinger equation for a 2D hydrogen atom are approximate solutions of (5) if $k_{\text{exc}} \ll k_{\Delta}$ that corresponds to $\alpha_c \ll 1$.

The dimensionless parameter α_c is the only parameter that governs physics of chiral excitons. It is approximately equal to the ratio between electron-hole Coulomb interaction energy and their kinetic energies. Experimentally relevant conditions³⁻⁵ correspond to the case $\alpha_c \ll 1$, therefore we use the analytical approximation described above for calculation of the optical conductivity tensor of a TI surface.

IV. OPTICAL CONDUCTIVITY TENSOR

For calculation of the optical conductivity tensor of a TI surface we used the linear response theory at zero temperature. Components of the conductivity can be written in a Lehmann representation in the following way:

$$\sigma_{\alpha\beta} = \frac{e^2}{\hbar} \sum_n \frac{i}{E_{n0}} \left(\frac{J_\alpha^{n0} J_\beta^{0n}}{\omega + E_{n0} + i\delta} + \frac{J_\alpha^{0n} J_\beta^{n0}}{\omega - E_{n0} + i\delta} \right), \quad (8)$$

where $|n\rangle$ and E_{n0} denote the excited state of the interacting system and its energy measured from the ground state $|0\rangle$ with filled valence band and empty conduction band; \mathbf{J} is the current operator in second quantization representation. Due to the momentum conservation law, only states $|n\rangle$ with zero momentum contribute to optical conductivity. Corresponding two-particle states of an interacting system include single-particle interband transitions $|n\rangle = a_{\mathbf{k}1}^+ a_{\mathbf{k}-1}|0\rangle$ and excitonic states $|n\rangle = d^+|0\rangle$. Their contributions to the optical conductivity tensor can be separated.

After substitution of single-particle sets of states $|n\rangle = a_{\mathbf{k}1}^+ a_{\mathbf{k}-1}|0\rangle$ into general formula (8) one can obtain the expression for the single-particle contribution to the optical conductivity tensor. The expression can be presented in the Kubo-Greenwood formula that is given by

$$\sigma_{\alpha\beta}^{\text{sp}} = \frac{e^2}{i\hbar} \sum_{\mathbf{k}\gamma\gamma'} \frac{n_{\mathbf{k}\gamma} - n_{\mathbf{k}\gamma'}}{\epsilon_{\mathbf{k}\gamma} - \epsilon_{\mathbf{k}\gamma'}} \frac{\langle f_{\mathbf{k}\gamma} | j_\alpha | f_{\mathbf{k}\gamma'} \rangle \langle f_{\mathbf{k}\gamma'} | j_\beta | f_{\mathbf{k}\gamma} \rangle}{\omega + \epsilon_{\mathbf{k}\gamma} - \epsilon_{\mathbf{k}\gamma'} + i\delta}. \quad (9)$$

Here $\mathbf{j} = v_F[\boldsymbol{\sigma} \times \mathbf{n}]$ is the single-particle current operator; and $n_{\mathbf{k}\gamma}$ is the occupation number of the corresponding state at zero temperature. After evaluation of (9) one can obtain

$$\begin{aligned} \text{Re}[\sigma_{xx}^{\text{sp}}] &= \frac{e^2}{\hbar} \frac{\pi}{8} \left[1 + \left(\frac{2\Delta}{\omega} \right)^2 \right] \Theta(|\omega| - 2|\Delta|), \\ \text{Im}[\sigma_{xx}^{\text{sp}}] &= \frac{e^2}{\hbar} \left[\frac{|\Delta|}{2\omega} + \left(\frac{1}{8} + \frac{\Delta^2}{2\omega^2} \right) \ln \left| \frac{\omega - 2|\Delta|}{\omega + 2|\Delta|} \right| \right], \end{aligned} \quad (10)$$

$$\begin{aligned} \text{Re}[\sigma_{yx}^{\text{sp}}] &= -\frac{e^2}{\hbar} \frac{\Delta}{2\omega} \ln \left| \frac{\omega - 2|\Delta|}{\omega + 2|\Delta|} \right|, \\ \text{Im}[\sigma_{yx}^{\text{sp}}] &= \frac{e^2}{\hbar} \frac{\pi \Delta}{2\omega} \Theta(|\omega| - 2|\Delta|). \end{aligned} \quad (11)$$

The obtained expressions for single-particle contribution to the optical conductivity tensor are the special case of more general formulas calculated within the quantum kinetic equation in Ref. 15 that takes into account disorder and finite temperature.

After substitution of the set of excitonic states d^+ to general formula (8) one can obtain the expression for the excitonic contribution to the optical conductivity tensor that have not yet been taken into account and can be presented in the following

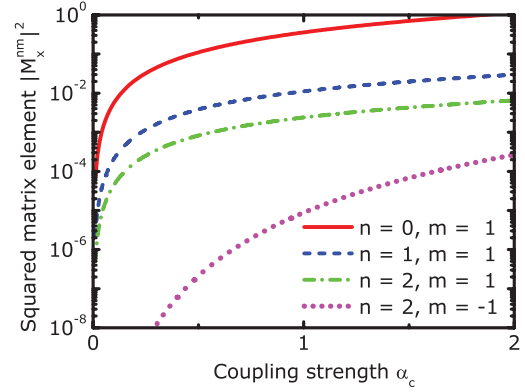


FIG. 1. (Color online) Squared dimensionless matrix element $|M_x^{nm}|^2$ for four lowest-energy optical active excitonic states ($|0, 1\rangle$, $|1, 1\rangle$, $|2, 1\rangle$, and $|2, -1\rangle$) as a function of dimensionless coupling α_c .

form:

$$\sigma_{xx}^{\text{exc}} = i \frac{e^2}{\hbar} \sum_{nm} |M_x^{nm}|^2 \frac{\omega + i\gamma}{\Omega_{nm}} \frac{2\Delta^2}{(\omega + i\gamma)^2 - \Omega_{nm}^2}, \quad (12)$$

$$\sigma_{yx}^{\text{exc}} = -\frac{e^2}{\hbar} \sum_{nm} m |M_x^{nm}|^2 \frac{2\Delta^2}{(\omega + i\gamma)^2 - \Omega_{nm}^2}. \quad (13)$$

Here the summation is performed over all exciton quantum numbers; γ is the phenomenologically introduced exciton decay rate; and \mathbf{M}^{nm} is the dimensionless matrix element that characterizes the coupling strength of the excitonic $|n, m\rangle$ level to the external electromagnetic field and depends only on dimensionless coupling strength α_c :

$$\mathbf{M}^{nm} = \frac{\hbar}{\Delta} \sum_{\mathbf{k}} C_{\mathbf{k}}^{nm} \langle \mathbf{k}, -1 | \mathbf{j} | \mathbf{k}, 1 \rangle. \quad (14)$$

Dimensionless matrix element \mathbf{M}^{nm} has a nonzero value only for levels with $m = \pm 1$ and all other states are optically inactive. Dependence of the squared matrix element $|M_x^{nm}|^2$ on dimensionless coupling strength for four optical active lowest-energy states is presented in Fig. 1. Absolute value of the matrix element $|\mathbf{M}^{nm}|$ is decreasing with the increasing of quantum number n due to destructive interference of single-particle states. Matrix element \mathbf{M}^{nm} consists of coherent superposition of single-particle matrix elements with weight functions $C_{\mathbf{k}}^{nm}$ and wave functions $C_{\mathbf{k}}^{nm}$ for high energy excitonic levels oscillate in momentum space. Also optical activity of the excitonic levels with orbital angular momentum $m = -1$ is considerably weaker than one for the levels with $m = 1$.

Contribution of the excitonic level $|n, m\rangle$ to Hall conductivity has the same sign as the orbital angular momentum quantum number m . States with opposite orbital angular momenta m and $-m$ are connected by the time reversal transformation. In conventional two- and three-dimensional insulators there is symmetry between states with opposite angular momenta ($\Omega_{nm} = \Omega_{n-m}$ and $|M_x^{nm}|^2 = |M_x^{n,-m}|^2$) due to time reversal symmetry. Therefore the total contribution of all excitonic states to Hall conductivity is zero. For chiral excitons on a TI surface with a magnetically opened gap the symmetry between states with opposite orbital angular momenta is broken and they *do* resonantly contribute to optical Hall conductivity.

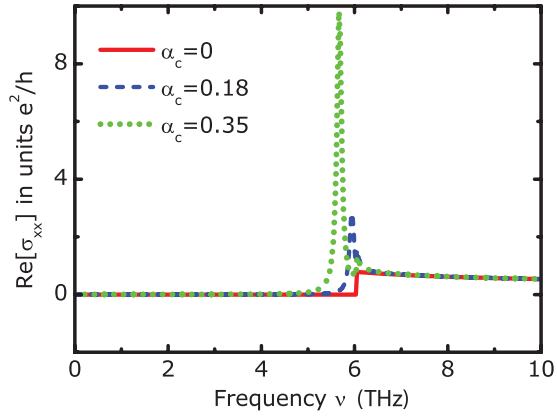


FIG. 2. (Color online) Frequency dependence of the real part of longitudinal conductivity $\text{Re}[\sigma_{xx}]$ for $\alpha_c = 0$ (solid red line), $\alpha_c = 0.18$ (dashed blue line), and $\alpha_c = 0.35$ (dotted green line).

For all numerical calculations we used the following parameters: $\Delta = 12.5$ meV, $\gamma = 0.25$ meV, and $v_F = 0.62 \times 10^6$ m/s. Also we used three values of dimensionless parameter α_c . Value $\alpha_c = 0$ corresponds to the case of noninteracting electrons on the TI surface. Values $\alpha_c = 0.18$ and $\alpha_c = 0.35$ correspond to values of effective permittivity $\epsilon = 20.5$ and $\epsilon = 10.5$, respectively. The value $\alpha_c = 0.18$ corresponds to Bi_2Te_3 and the other values of α_c are used for comparison.

Real parts of longitudinal and Hall components of the optical conductivity tensor $\text{Re}[\sigma_{xx}(\omega)]$ and $\text{Re}[\sigma_{yx}(\omega)]$ are represented in Figs. 2 and 3, respectively. At low frequencies contribution of excitons can be neglected and the conductivity tensor tends to its single-particle value [Eqs. (10) and (11)]. Chiral excitons correspond to a sharp maximum of longitudinal conductivity that leads to resonant absorption of energy of an electromagnetic wave. For the used set of parameters the only maximum can be distinguished and corresponds to the excitonic level $|0,1\rangle$ and the contribution of other excitonic levels almost merges with a contribution of single-particle transitions. Contrary to conventional ones, chiral excitons resonantly contribute to Hall conductivity and, hence, can play an important role in Faraday and Kerr effects.

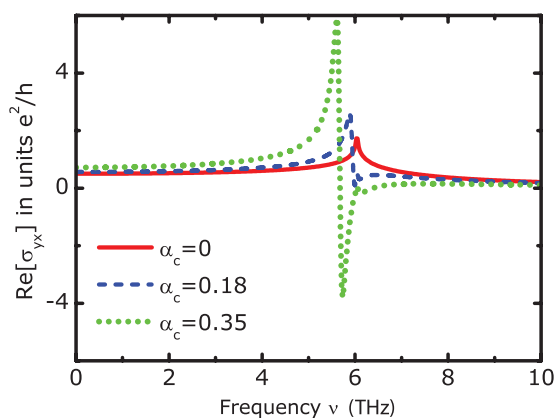


FIG. 3. (Color online) Frequency dependence of the real part of Hall conductivity $\text{Re}[\sigma_{yx}]$ for $\alpha_c = 0$ (solid red line), $\alpha_c = 0.18$ (dashed blue line), and $\alpha_c = 0.35$ (dotted green line).

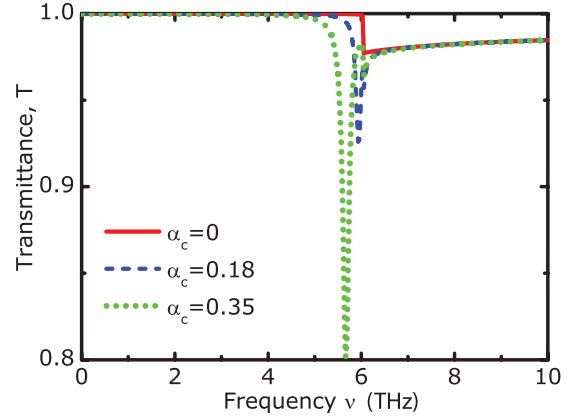


FIG. 4. (Color online) Frequency dependence of transmittance T through TI thin film for $\alpha_c = 0$ (solid red line), $\alpha_c = 0.18$ (dashed blue line), and $\alpha_c = 0.35$ (dotted green line).

V. FARADAY AND KERR EFFECTS IN TI THIN FILM

We consider Faraday and Kerr effects at normal incidence of an electromagnetic wave in thin films of TIs whose width is less than the wavelength. Our results can be easily generalized to more complicated geometry and oblique incidence.

If an incident electromagnetic wave is linearly polarized $\mathbf{E} = \mathbf{e}_x E_0$, where E_0 is its amplitude, characteristics of transmitted and reflected waves can be expressed in terms of amplitudes of transmission $t_\lambda = |t_\lambda| e^{i\Phi_\lambda^t}$ and reflection $r_\lambda = |r_\lambda| e^{i\Phi_\lambda^r}$ of a circularly polarized electromagnetic wave $\mathbf{E} = (\mathbf{e}_x + i\lambda \mathbf{e}_y) E_0$, where $\lambda = \pm 1$ is the sign of the circular polarization. Transmittance of an electromagnetic wave through the TI film is given by $T = (|t_+|^2 + |t_-|^2)/2$. The angle of polarization plane rotation (Faraday angle) θ_F and ellipticity δ_F of the transmitted wave are given by $\theta_F = (\Phi_+^t - \Phi_-^t)/2$ and $\delta_F = (|t_+| - |t_-|)/(|t_+| + |t_-|)$, respectively. The angle of polarization plane rotation (Kerr angle) θ_K and ellipticity δ_K of the reflected wave are given by $\theta_K = (\Phi_+^r - \Phi_-^r)/2$ and $\delta_K = (|r_+| - |r_-|)/(|r_+| + |r_-|)$, respectively.

Using Maxwell equations for thin film geometry and the boundary conditions for electric and magnetic fields that take into account electric currents excited by electromagnetic

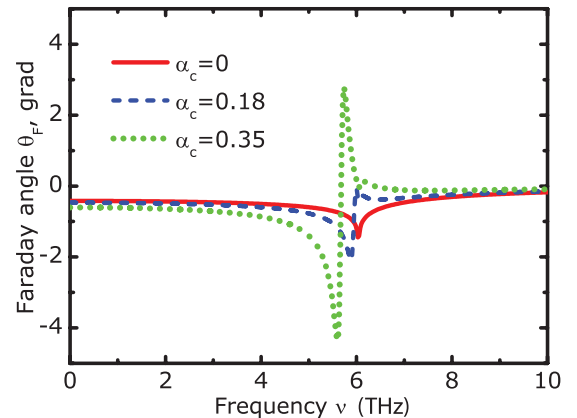


FIG. 5. (Color online) Frequency dependence of Faraday angle θ_F for $\alpha_c = 0$ (solid red line), $\alpha_c = 0.18$ (dashed blue line), and $\alpha_c = 0.35$ (dotted green line).

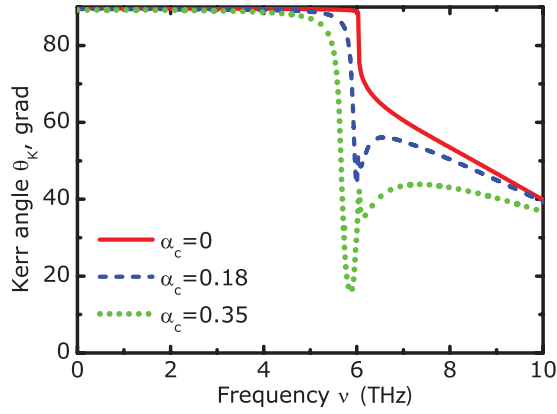


FIG. 6. (Color online) Frequency dependence of Kerr angle θ_K for $\alpha_c = 0$ (solid red line), $\alpha_c = 0.18$ (dashed blue line), and $\alpha_c = 0.35$ (dotted green line).

waves, we find

$$t_\lambda = \frac{\sigma_0}{\sigma_0 + \alpha\sigma_\lambda^t}, \quad r_\lambda = -\frac{\alpha\sigma_\lambda^t}{\sigma_0 + \alpha\sigma_\lambda^t}, \quad (15)$$

where $\sigma_0 = e^2/h$ is the quantum of conductivity; $\alpha \approx 1/137$ is the fine structure constant; $\sigma_\lambda^t = \sigma_{xx}^t + i\lambda\sigma_{yx}^t$; and $\sigma_{\alpha\beta}^t$ is the sum of the optical conductivity components from the opposite surfaces of the TI film. The direction of the polarization plane rotations for reflected and transmitted electromagnetic waves depends on the sign of the Hall conductivity and, hence, on the sign of the z component of the exchange field. The rotations on the opposite surfaces of the TI film enhance each other if the sign of the corresponding component of the exchange fields on opposite surfaces coincide. The case is considered below. If also the absolute values of the magnetically induced gaps on the opposite surfaces are the same then $\sigma_{\alpha\beta}^t = 2\sigma_{\alpha\beta}$. If the corresponding components of the exchange fields have different signs and the same absolute values then $\sigma_{\alpha\beta}^t = 0$ and Faraday and Kerr effects vanish.

Dependence of transmittance T of the electromagnetic wave through the TI thin film on its frequency ω is represented in Fig. 4. Chiral excitonic levels lead to resonant absorption of energy of the electromagnetic wave. But absorption of

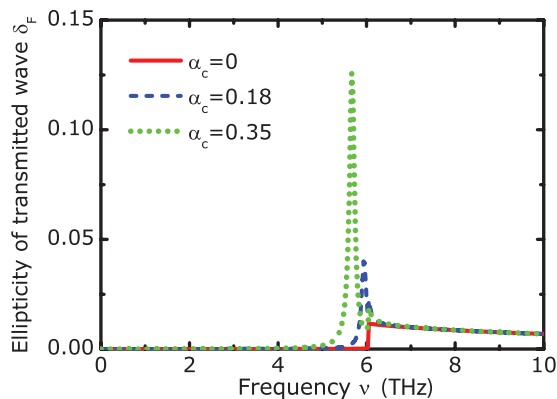


FIG. 7. (Color online) Frequency dependence of ellipticity of transmitted wave δ_F for $\alpha_c = 0$ (solid red line), $\alpha_c = 0.18$ (dashed blue line), and $\alpha_c = 0.35$ (dotted green line).

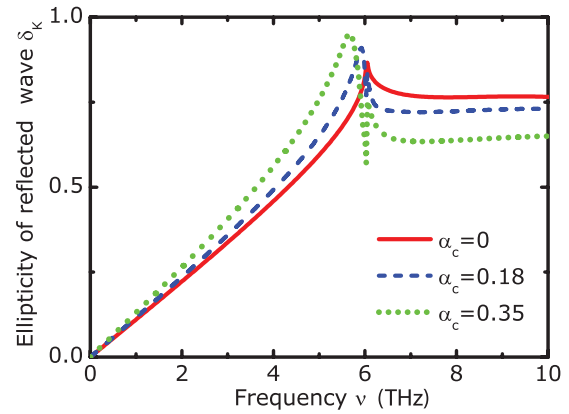


FIG. 8. (Color online) Frequency dependence of ellipticity of reflected wave δ_K for $\alpha_c = 0$ (solid red line), $\alpha_c = 0.18$ (dashed blue line), and $\alpha_c = 0.35$ (dotted green line).

energy is too small to prevent detection of the transmitted electromagnetic wave.²⁵

Dependence of Faraday angle θ_F and Kerr angle θ_K on the frequency ω is presented in Figs. 5 and 6. At low frequencies contribution of excitons to optical conductivity is insignificant and Faraday θ_F and Kerr angles θ_K tend to their universal values $\tan \theta_F = \alpha$ and $\tan \theta_K = 1/\alpha$, respectively, where $\alpha \approx 1/137$ is a fine structure constant. Resonance enhancement of Hall conductivity by chiral excitons leads to resonant enhancement of the Faraday angle. The Kerr angle is very sensitive to the longitudinal component of the conductivity tensor.²⁶ At the resonant condition the longitudinal component of the optical conductivity has a sharp peak and, hence, the Kerr angle is considerably reduced. Both of these prominent effects can be directly observed in experiment.

Dependence of the ellipticities of transmitted δ_F and reflected δ_K electromagnetic waves are presented in Figs. 7 and 8. Chiral excitons resonantly enhance ellipticity of the transmitted wave δ_F and lead to observable signature in ellipticity δ_K of the reflected wave. These signatures can also be directly observed in the experiments.

VI. CONCLUSIONS

Resonant features in Faraday and Kerr effects caused by chiral excitons in thin TI film can be observable in experiments if contribution of at least a single excitonic level to Hall conductivity is well separated from single-particle contribution. Thus the excitonic binding energy $\Omega_b = \alpha_c^2 |\Delta|$ of the lowest energy state $|0, 1\rangle$ should exceed the excitonic decay rate γ . The maximal value of the gap induced in Bi_2Se_3 by ordered magnetic impurities⁹ is $2|\Delta| \approx 50$ meV. For Bi_2Se_3 the dimensionless coupling constant and the binding energy are $\alpha_c = 0.09$ and $\Omega_b \sim 2$ K. For Bi_2Te_3 the dimensionless coupling constant and the binding energy are $\alpha_c = 0.18$ and $\Omega_b \sim 9$ K. Exciton decay rate γ can be estimated from the scattering rate of electrons. Maximal value of the electron mobility in absence of the gap estimated from transport experiments² is $\mu \sim 10^4$ cm²/eVs. It corresponds to the scattering rate $\gamma \sim 30$ K, hence, present parameters relevant to the experiments are close enough to the favorable ones.

The dielectric constant of bismuth and telluride based TI achieves $\epsilon \approx 40\text{--}100$, hence the coupling constant and exciton binding energies of the chiral exciton energies are rather small. So resonant excitonic resonances are fragile to disorder and finite temperature effects. The problem can be overcome in ultrathin TI films whose width is considerably less than the exciton radius $k_{\text{exc}}d \ll 1$. In that case the effective dielectric constant of a TI film equals the half-sum of the dielectric constant of a substrate surrounding the film and does not depend on one of the TI. Its value can be considerably smaller than the dielectric permittivity of the TI. For $\alpha_c = 0.18$ the character value of d equals 60 nm.

We used the Hartree-Fock approximation for the description of the delocalized single-particle states. In this approximation correlation between the motion of the electron and hole is neglected and their wave functions are approximated by independent plane waves. So Coulomb interaction leads only to renormalization of single-particle spectrum. Correlations for delocalized electron-hole states (unbound excitons) in a more complicated approximation (that involves the calculation of a two-particle Green function) were considered for conventional semiconductor nanostructures (see Refs. 27,28, and references therein). Coulomb interaction leads to enhancement of the absorption spectrum with the Sommerfeld-Gamov factor. But in any case single-particle contribution is not the resonant and it is smooth as a function of frequency. Hence if the chiral excitonic state on a TI surface is well separated from the continuum of single-particle transitions ($\omega \geq 2|\Delta|$) the resonant Faraday and Kerr effects will be observable.

Chiral excitons also appear²¹ in monolayer and bilayer graphene. In the former the gap in the spectrum can be induced by the special substrate, for example BN²⁹ or SiC.³⁰ The spectrum in the latter can be gapped by the external electric field perpendicular to the layer.^{22–24} The chiral excitonic state with minimal energy in monolayer and bilayer graphene has orbital angular momentum $m = 1$ and $m = 2$, respectively. In the first Brillouin zone of both materials there are two valleys connected with each other by the time reversal transformation.⁸ Due to the time reversal symmetry the value of the gaps in the two valleys have exactly the same absolute values and opposite signs $|\Delta|$ and $-|\Delta|$. The chiral excitons from the single valley resonantly contribute to the optical Hall conductivity, but the contributions of the two valleys cancel each other. Therefore the chiral excitons in gapped monolayer and bilayer graphene do not manifest in Faraday and Kerr effects in the absence of the external magnetic field.

The time reversal symmetry on a surface of TI can be also broken by an external magnetic field perpendicular to the surface leading to reconstruction of the Dirac spectrum

to separate Dirac Landau levels.^{1,2} Optical Hall conductivity consists of the set of resonances that correspond to optical single-particle transitions between Dirac Landau levels.¹⁴ In the presence of the Coulomb interaction, energy of single-particle transition depends on its total momentum and the set of Landau levels transforms to the set of the dispersive magnetoexcitonic branches.^{31–37} Only magnetoexcitons with zero total momentum contribute to the optical conductivity tensor, hence Coulomb interaction does not qualitatively change frequency dependence of Hall conductivity. Coulomb interaction shifts the positions of the resonances and can change their amplitudes. Manifestation of magnetoexcitons in Faraday and Kerr effects is not so prominent as chiral excitons on a TI surface with the magnetically induced gap.

At present Faraday and Kerr effects in thin TI films subjected to an external perpendicular magnetic field are extensively studied experimentally.^{38–41} Real samples contain residual bulk charge carriers (that are not completely excluded by doping) and polar phonons interacting with electromagnetic waves. Complicated dependencies of Kerr and Faraday angles and peaks in longitudinal conductivity observed in Refs. 38–41 are interpreted in terms of bulk response. Observed signatures that do not depend on TI film thickness can be caused by magnetoexcitons.

In summary, we theoretically investigated the manifestations of chiral excitons on the magnetically gapped surfaces of topological insulator film in Faraday and Kerr effects. Contribution of chiral excitons to optical conductivity tensor of the TI surface is calculated. As conventional excitons chiral ones lead to a sharp peak of longitudinal conductivity and to resonance absorption of energy of incident electromagnetic wave. Contrary to conventional excitons chiral ones due to lack of symmetry between states with opposite angular momentum resonantly enhance Hall conductivity and play an important role in Faraday and Kerr effects. Chiral excitons lead to considerable enhancement of Faraday angle and ellipticity of transmitted electromagnetic waves at resonance condition. Also they lead to resonant weakening of the Kerr angle and prominent signatures in ellipticity of reflected electromagnetic waves. The described effects can be directly observed in the experiments.

ACKNOWLEDGMENTS

The authors are indebted to A. A. Sokolik for fruitful discussions. The work was supported by RFBR programs. D.K.E acknowledges support from the Grant of the President of Russian Federation MK-5288.2011.2, RFBR Grant 12-02-31199, and by a scholarship from the Dynasty Foundation.

*lozovik@isan.troitsk.ru

¹M. Z. Hasan and C. L. Kane, *Rev. Mod. Phys.* **82**, 3045 (2010).

²X. L. Qi and S. C. Zhang, *Rev. Mod. Phys.* **83**, 1057 (2011).

³Y. L. Chen *et al.*, *Science* **325**, 178 (2009).

⁴P. Roushan, J. Seo, C. V. Parker, Y. S. Hor, D. Hsieh, D. Qian, A. Richardella, M. Z. Hasan, R. J. Cava and A. Yazdani, *Nature (London)* **460**, 1106 (2009).

⁵Y. Xia *et al.*, *Nat. Phys.* **5**, 398 (2009).

⁶K. S. Novoselov, A. K. Geim, S. V. Morozov, D. Jiang, Y. Zhang, S. V. Dubonos, I. V. Grigorieva, and A. A. Firsov, *Science* **306**, 666 (2004).

⁷K. S. Novoselov, A. K. Geim, S. V. Morozov, D. Jiang, M. I. Katsnelson, I. V. Grigorieva, S. V. Dubonos, and A. A. Firsov, *Nature (London)* **438**, 197 (2005).

- ⁸A. H. Castro Neto, F. Guinea, N. M. R. Peres, K. S. Novoselov, and A. K. Geim, *Rev. Mod. Phys.* **81**, 109 (2009).
- ⁹Y. L. Chen *et al.*, *Science* **329**, 659 (2010).
- ¹⁰L. A. Wray, S.-Y. Xu, Y. Xia, D. Hsieh, A. V. Fedorov, Y. S. Hor, R. J. Cava, A. Bansil, H. Lin, and M. Z. Hasan, *Nat. Phys.* **7**, 32 (2011).
- ¹¹I. Garate and M. Franz, *Phys. Rev. B* **84**, 045403 (2011).
- ¹²J. Maciejko, X. L. Qi, H. D. Drew, and S. C. Zhang, *Phys. Rev. Lett.* **105**, 166803 (2010).
- ¹³Y. Lan, S. Wan, and S. C. Zhang, *Phys. Rev. B* **83**, 205109 (2011).
- ¹⁴W.-K. Tse and A. H. MacDonald, *Phys. Rev. B* **82**, 161104 (2010).
- ¹⁵W.-K. Tse and A. H. MacDonald, *Phys. Rev. Lett.* **105**, 057401 (2010).
- ¹⁶X. L. Qi, T. L. Hughes, and S. C. Zhang, *Phys. Rev. B* **78**, 195424 (2008).
- ¹⁷A. M. Essin, J. E. Moore, and D. Vanderbilt, *Phys. Rev. Lett.* **102**, 146805 (2009).
- ¹⁸F. Wilczek, *Phys. Rev. Lett.* **58**, 1799 (1987).
- ¹⁹T. Misawa, T. Yokoyama, and S. Murakami, *Phys. Rev. B* **84**, 165407 (2011).
- ²⁰I. Egri, *Phys. Rep.* **119**, 363 (1985).
- ²¹C. H. Park and G. Louie, *Nano. Lett.* **10**, 426 (2010).
- ²²E. McCann, *Phys. Rev. B* **74**, 161403 (2006).
- ²³K. S. Novoselov, E. McCann, S. V. Morozov, V. I. Falko, M. I. Katsnelson, U. Zeitler, D. Jiang, F. Schedin, and A. K. Geim, *Nat. Phys.* **2**, 177 (2006).
- ²⁴Y. Zhang, T.-T. Tang, C. Girit, Z. Hao, M. C. Martin, A. Zettl, M. F. Crommie, Y. R. Shen, and F. Wang, *Nature (London)* **459**, 820 (2009).
- ²⁵In real samples Bi_2Se_3 and Bi_2Te_3 are inevitable bulk charge carriers and polar phonons that also lead to absorption of energy.
- ²⁶G. Tkachov and E. M. Hankiewicz, *Phys. Rev. B* **84**, 035405 (2011).
- ²⁷R. J. Elliot, *Phys. Rev.* **108**, 1384 (1957).
- ²⁸S. Glutch, *Excitons in Low-Dimensional Semiconductors: Theory, Numerical Methods, Applications* (Springer, Berlin, 2004).
- ²⁹G. Giovannetti, P. A. Khomyakov, G. Brocks, P. J. Kelly, and J. van den Brink, *Phys. Rev. B* **76**, 073103 (2007).
- ³⁰S. Y. Zhou, G.-H. Gweon, and A. V. Fedorov, *Nat. Mater.* **6**, 770 (2007).
- ³¹C. Kallin and B. I. Halperin, *Phys. Rev. B* **30**, 5655 (1984).
- ³²I. V. Lerner and Yu. E. Lozovik, *Sov. Phys. JETP* **51**, 588 (1980); **53**, 763 (1981).
- ³³A. B. Dzubenko and Yu. E. Lozovik, *J. Phys. A: Math. Gen.* **24**, 415 (1991).
- ³⁴S. A. Moskalenko, M. A. Liberman, P. I. Khadzi, E. V. Dumanov, I. V. Podlesny, and V. Botan, *Solid State Commun.* **140**, 236 (1996).
- ³⁵Z. G. Koinov, *Phys. Rev. B* **79**, 073409 (2009).
- ³⁶A. A. Pikalov and D. V. Fil, *Nanoscale Res. Lett.* **7**, 145 (2012).
- ³⁷Yu. E. Lozovik and A. A. Sokolik, *Nanoscale Res. Lett.* **7**, 134 (2012).
- ³⁸G. S. Jenkins, A. B. Sushkov, D. C. Schmadel, N. P. Butch, P. Syers, J. Paglione, and H. D. Drew, *Phys. Rev. B* **82**, 125120 (2010).
- ³⁹J. A. Sobota, S. Yang, J. G. Analytis, Y. L. Chen, I. R. Fisher, P. S. Kirchmann, and Z.-X. Shen, *Phys. Rev. Lett.* **108**, 117403 (2012).
- ⁴⁰J. N. Hancock, J. L. M. van Mechelen, A. B. Kuzmenko, D. van der Marel, C. Brune, E. G. Novik, G. V. Astakhov, H. Buhmann, and L. W. Molenkamp, *Phys. Rev. Lett.* **107**, 136803 (2011).
- ⁴¹R. Valdes Aguilar *et al.*, *Phys. Rev. Lett.* **108**, 087403 (2012).